JACS
JOURNAL OF THE AMERICAN CHEMICAL SOCIETY
pubs.acs.org/JACS
Article

Isosteric 3D Bicyclo[1.1.1]Pentane (BCP) Core-Based Lipids for mRNA Delivery and CRISPR/Cas Gene Editing

Shiying Wu, Yangyang Yang, Xizhen Lian, Fangyu Zhang, Chao Hu, Jet Tsien, Zexiang Chen, Yehui Sun, Amogh Vaidya, Minjeong Kim, Yun-Chieh Sung, Yufen Xiao, Xiaoyan Bian, Xu Wang, Zeru Tian, Erick Guerrero, Joshua Robinson, Pratima Basak, Tian Qin,* and Daniel J. Siegwart*

Cite This: J. Am. Chem. Soc. 2024, 146, 34733−34742
Read Online

ABSTRACT: Lipid nanoparticles (LNPs) are an essential component of messenger RNA (mRNA) vaccines and genome editing therapeutics. Ionizable amino lipids, which play the most crucial role in enabling mRNA to overcome delivery barriers, have, to date, been restricted to two-dimensional (2D) architectures. Inspired by improved physicochemical properties resulting from the incorporation of three-dimensionality (3D) into small-molecule drugs, we report the creation of 3D ionizable lipid designs through the introduction of bicyclo[1.1.1]pentane (BCP) core motifs. BCP-based lipids enabled efficient *in vivo* mRNA delivery to the liver and spleen with significantly greater performance over 2D benzene- and cyclohexane-based analogues. Notably, lead BCP-NC2-C12 LNPs mediated ∼90% reduction in the PCSK9 serum protein level via CRISPR/Cas9 gene knockout, outperforming 2D controls and clinically used DLin-MC3-DMA LNPs at the same dose. Here, we introduce BCP-based designs with superior *in vivo* activity, thereby expanding the chemical scope of ionizable amino lipids from 2D to 3D and offering a promising avenue to improve mRNA and gene editing efficiency for the continued development of genetic medicines.

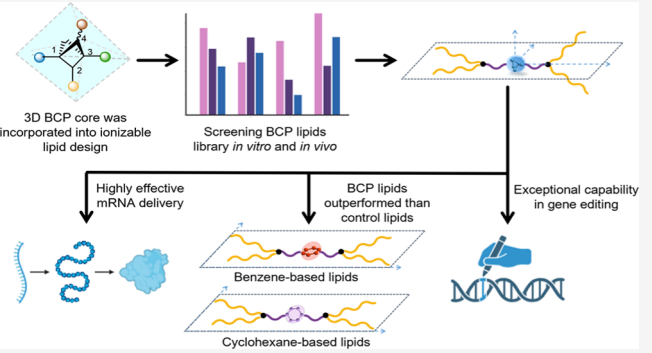

INTRODUCTION

Messenger RNA (mRNA) has emerged as a promising platform for broad medical applications including vaccines, protein replacement therapies, cancer immunotherapies, and genome editing.[1−13] The remarkable and life-saving success of the COVID-19 mRNA vaccines (Comirnaty from Pfizer/BioNTech and Spikevax from Moderna),[14,15] which were enabled through lipid nanoparticle (LNP) delivery, highlights the essential role that LNPs play in overcoming delivery barriers. LNPs are typically composed of ionizable amino lipids, phospholipids, cholesterol, and PEGylated lipids.[16−26] Among these constituents, ionizable amino lipids are the most essential, as their unique pH-responsive behavior and membrane-disruptive properties overcome the key barriers of mRNA delivery, including mRNA encapsulation, cellular uptake, and endosomal escape.[4,19,27] The chemical structures of ionizable amino lipids have to date been restricted to two-dimensional (2D) architectures.[25,28] Meanwhile, in the field of small-molecule drug development, the incorporation of three-dimensionality (3D) has recently made a major clinical impact through improving solubility, structural conformation, and drug pocket binding of small-molecule drugs.[29−35] Inspired by the success and improved physical properties of 3D architectures, we herein report the creation of 3D ionizable lipid designs based on a bicyclo[1.1.1]pentane (BCP) scaffold. By expanding the chemical scope of ionizable amino lipids from 2D to 3D, BCP-based lipids offer a new direction for the continued development of genetic medicines.

The realm of small-molecule drugs is rich in chemical complexity, which can inspire the design of novel ionizable amino lipids. Cyclic structures, especially benzene, are ubiquitous structural motifs for small-molecule drugs owing to structural rigidity, high bioactivities, and substituent effect enabling structure−activity relationship (SAR) studies.[36−41] However, benzenes are also frequently associated with poor drug-like properties including metabolic instability and poor aqueous solubility.[42−45] Recent developments in medicinal chemistry have demonstrated that substituting benzene rings with BCP[46,47] can enhance the pharmacokinetic/pharmacodynamic (PK/PD) performance, improve safety profiles, and increase the biological activity of small-molecule drugs via

Received: September 20, 2024
Revised: November 25, 2024
Accepted: November 27, 2024
Published: December 10, 2024

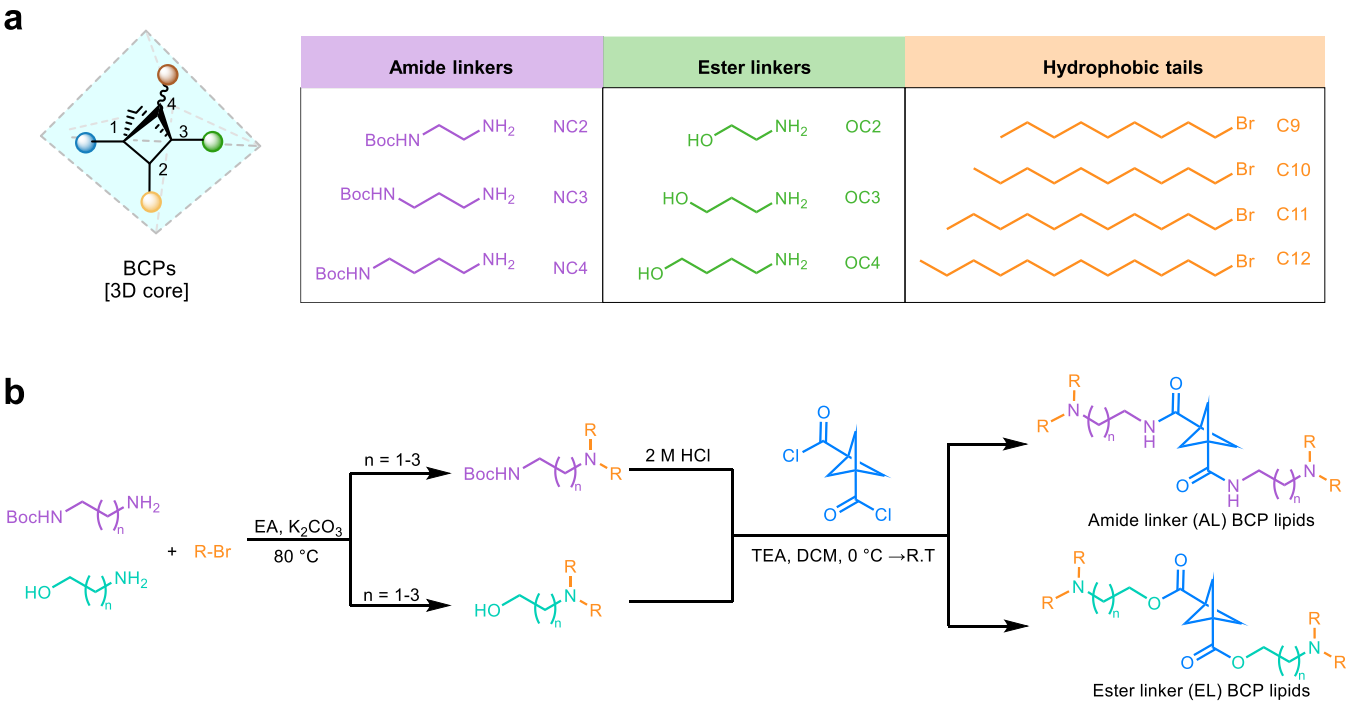

Figure 1. Modular synthetic routes were employed to synthesize a systematic series of ionizable amino BCP lipids for mRNA delivery. (a) Unique 3D structure of the BCP core, ALs and ELs, and alkyl tail-forming building blocks. (b) Parallel synthetic routes enabling the concise synthesis of AL and EL containing BCP lipids.

increasing solubility, metabolic stability, and membrane fusion capabilities.[31,34,42,45−47] Furthermore, recent synthetic advances provided multiple practical approaches to accessing strained BCP motifs.[48−58] Extrapolating from small-molecule drug development, we hypothesized that introducing the 3D BCP core into an ionizable lipid design could provide improved delivery efficiency. Since ionizable amino lipids reported previously were primarily based on 2D cores, this new BCP approach greatly expands the chemical space for the design and application of ionizable lipids in LNPs. Herein, we designed and synthesized a systematic series of BCP lipids (Figure 1), containing four parts: (i) a compact and rigid 3D BCP core in the center; (ii) biodegradable amide linkers (ALs) or ester linkers (ELs) to connect the core and hydrophobic domain; (iii) tertiary amine head groups to increase affinity with nucleic acid and promote the self-assembly of nanoparticles; and (iv) hydrophobic tails to contribute to lipid bilayer construction, LNP stability, and transfection efficiency. BCP lipids with ALs preferred to transfect the liver, whereas BCP lipids with ELs preferred to transfect the spleen following intravenous (IV) administration of luciferase mRNA LNPs. Importantly, 3D BCP lipids demonstrated significantly greater mRNA delivery efficiency *in vitro* and *in vivo* than analogous 2D lipids composed of benzene or cyclohexane cores. Notably, compared to DLin-MC3-DMA (MC3) LNPs, which are used clinically to treat liver disease,[59] the mRNA transfection efficiency of BCP-NC2-C12 LNPs in the liver was 25 times that of the former. Additionally, we employed BCP LNPs to codeliver Cas9 mRNA and guide RNA for *Pcsk9* gene knockout and achieved over 90% reduction of PCSK9 protein production in the serum. This result for 3D BCP-NC2-C12 LNPs was around 3-fold greater than 2D-core LNPs and benchmark MC3 LNPs. Overall, this work demonstrates the superiority of 3D core integration, opening new avenues for creative lipid design with improved mRNA and gene editing efficiency for the continued development of genetic medicines.

RESULTS AND DISCUSSION

Design and Synthesis of BCP Lipids. BCP has emerged as the most useful bioisostere of benzene rings for small-molecule drugs. In 2012, Pfizer researchers improved the γ-secretase inhibitor BMS-708,163 by replacing its benzene ring with a BCP, enhancing its solubility, permeability, and stability.[46] Similarly, darapladib, an inhibitor of lipoprotein-associated phospholipase A2 (LpPLA2), uses BCP to achieve high potency and better physicochemical properties.[47] To introduce the 3D architecture into ionizable amino lipids, we developed modular synthetic routes using BCP as a core-forming motif. BCP, as a highly strained polycyclic hydrocarbon, may contribute to more stable, well-organized LNPs with improved encapsulation efficiency and delivery efficacy. Since linker chemistry has been shown to affect the performance and biodistribution of LNPs in previous studies,[25,60,61] we installed biodegradable ALs (NC2, NC3, and NC4) and ELs (OC2, OC3, and OC4) of varying lengths to the bridgehead 1,3-positions of BCPs. Additionally, inspired by previous studies showing the observable impact of alkyl tail length on the efficacy of LNPs, hydrophobic tails with various lengths (C9−C12) were linked with terminal amines via systematic conjugation.[25,60,62,63] We therefore varied the hydrophobic tail lengths (C9, C10, C11, and C12) through systematic conjugation to the tertiary amine. The eventual design ensured two tertiary amine heads in the BCP lipids for high affinity with nucleic acid cargoes and a tendency to self-assemble into nanoparticles (Figure 1a). A modular synthetic route to access BCP lipids effectively, beginning with the alkylation of amines followed by subsequent esterification or deprotection and amide coupling reaction, built up a library

https://doi.org/10.1021/jacs.4c13154
J. Am. Chem. Soc. 2024, 146, 34733−34742

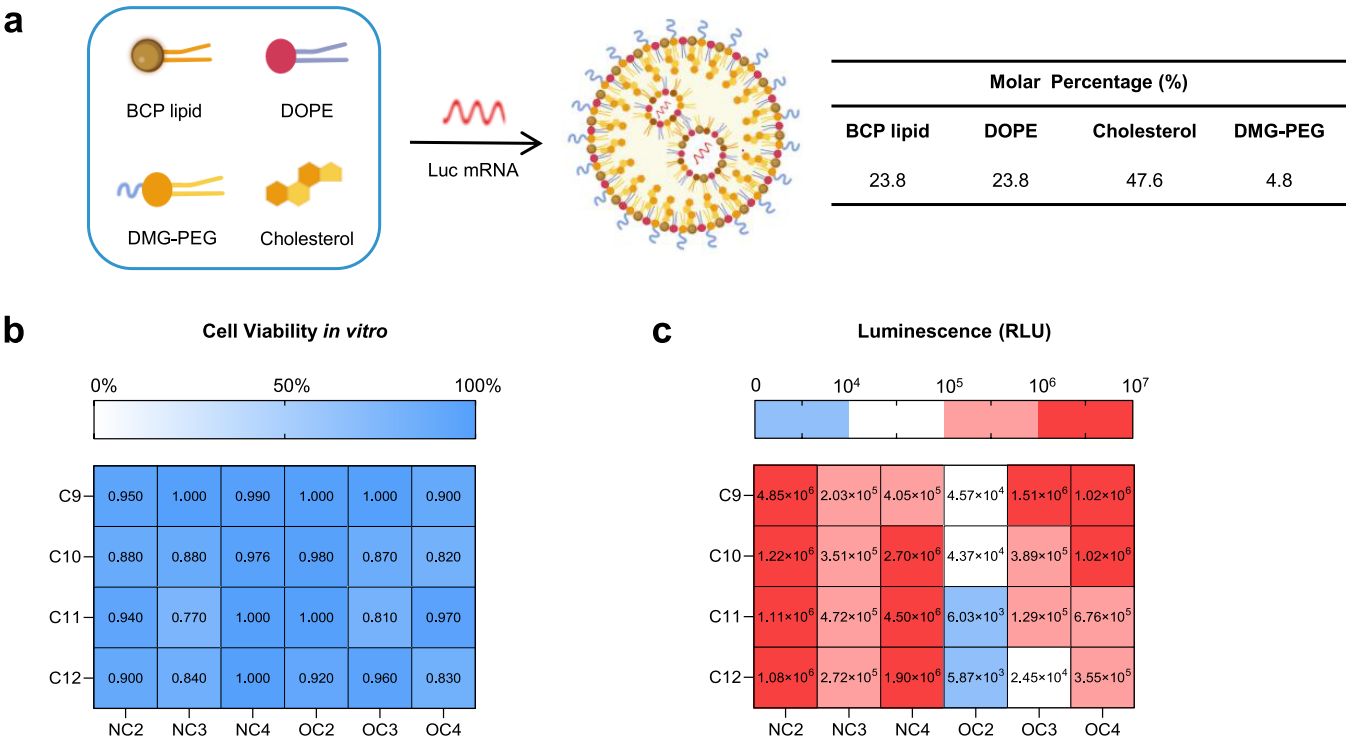

Figure 2. BCP LNPs were formulated with mRNA and characterized. (a) Luc mRNA LNPs consisting of BCP-based lipids, DOPE, cholesterol, and DMG-PEG were prepared by using the ethanol dilution method. Heat maps of (b) cell viability and (c) relative light units of IGROV-1 cells after treatment with BCP LNPs (25 ng mRNA/well, $n = 4$).

containing 24 BCP lipids for systematic structural−activity relationship studies (Figure 1b). In the first synthetic step, amide or ELs reacted with bromoalkanes through SN2 reaction under basic conditions in ethyl acetate to obtain the intermediate compounds, with a yield of around 80% after 48 h of reaction time (Schemes S1 and S2). Subsequently, the intermediate compounds were reacted with BCP acyl chloride for amide coupling or esterification with triethylamine as the base in dichloromethane, yielding approximately 75% yield of desired products (Schemes S3−S13). The final products were purified by chromatography using silica gel and confirmed by high-resolution mass spectroscopy, ^{1}H NMR, and ^{13}C NMR (Supporting Information). To compare 3D and 2D lipids head-to-head, we synthesized analogous 2D-core ionizable lipids using para-substituted benzene as the core motif via similar synthetic routes, as well as their saturated analogues containing *cis*-cyclohexane (*cis*-H) and *trans*-cyclohexane (*trans*-H) core scaffolds (Schemes S3−S13). Through the above-described synthetic routes, BCP lipids and 2D-core lipids were synthesized in scalable reactions, which are essential for LNP manufacturing.

BCP LNPs Effectively Encapsulated and Delivered mRNA. Following the designed synthetic route, all BCP lipids were successfully obtained (Figure S1). LNPs were formulated using a four-lipid mixture containing BCP lipids, 1,2-dioleoyl-snglycero-3-phosphoethanolamine (DOPE), cholesterol, and 1,2-dimyristoyl-rac-glycerol-methoxy(poly(ethylene glycol)) (DMG-PEG) with a molar percentage of 23.8/23.8/47.6/4.8 to mirror a previous study that optimized LNP formulations for mRNA.[64] Established protocols for LNP self-assembly with firefly luciferase (Luc) mRNA and characterization were followed, as previously reported (Figure 2a).[64] BCP lipids are named according to the core-forming motif (BCP, benzene, *cis*-H, *trans*-H), the linker (NC2−NC4, OC2−OC4), and the tail (C9−C12). In all comparison studies, all LNP components and ratios remained constant except for the ionizable amino lipid. The hydrodynamic diameter, polydispersity index (PDI), and mRNA encapsulation efficiency of resulting BCP LNPs were determined using dynamic light scattering and the RiboGreen assay following standardized protocols.[64] The hydrodynamic diameter of all BCP LNPs fell in the range of 120−180 nm, similar to previous studies, and exhibited a PDI below 0.17 (Figure S2a).[3,64,65] All BCP LNPs effectively encapsulated mRNA with efficiency values ranging from 80 to 98% (Figure S2b). We next evaluated the *in vitro* mRNA delivery efficiency and cytotoxicity of BCP LNPs in a cell culture. Luc mRNA was encapsulated in BCP LNPs and delivered to IGROV-1 cells. Minimal cytotoxicity was measured, with the majority of BCP LNPs demonstrating >90% viability after 24 h of incubation at the tested dose (Figure 2b). Regarding trends related to the linker length and chemistry, NC2, NC4, OC3, and OC4 linker-containing BCP LNPs most effectively delivered mRNA with the relative luminescence intensity ranging from 10^5 to 10^7 photons/s (Figure 2c). To further examine the potential compatibility of BCP lipids, we examined alternative phospholipids (DOPC, POPC, and POPE) and molar ratio compositions associated with the delivery of small or large RNAs (Figure S12). The activity was preserved across the formulations, highlighting the modularity of BCP lipids. High cell viability was also quantified in comparison to commercial LNP formulations, indicating favorable safety profiles (Figure S13). With these promising *in vitro* results of BCP LNPs, we next investigated their performance *in vivo*.

BCP LNPs Enabled Highly Effective mRNA Delivery In Vivo. We dosed C57BL6 mice with 0.1 mg/kg Luc mRNA

https://doi.org/10.1021/jacs.4c13154
J. Am. Chem. Soc. 2024, 146, 34733−34742

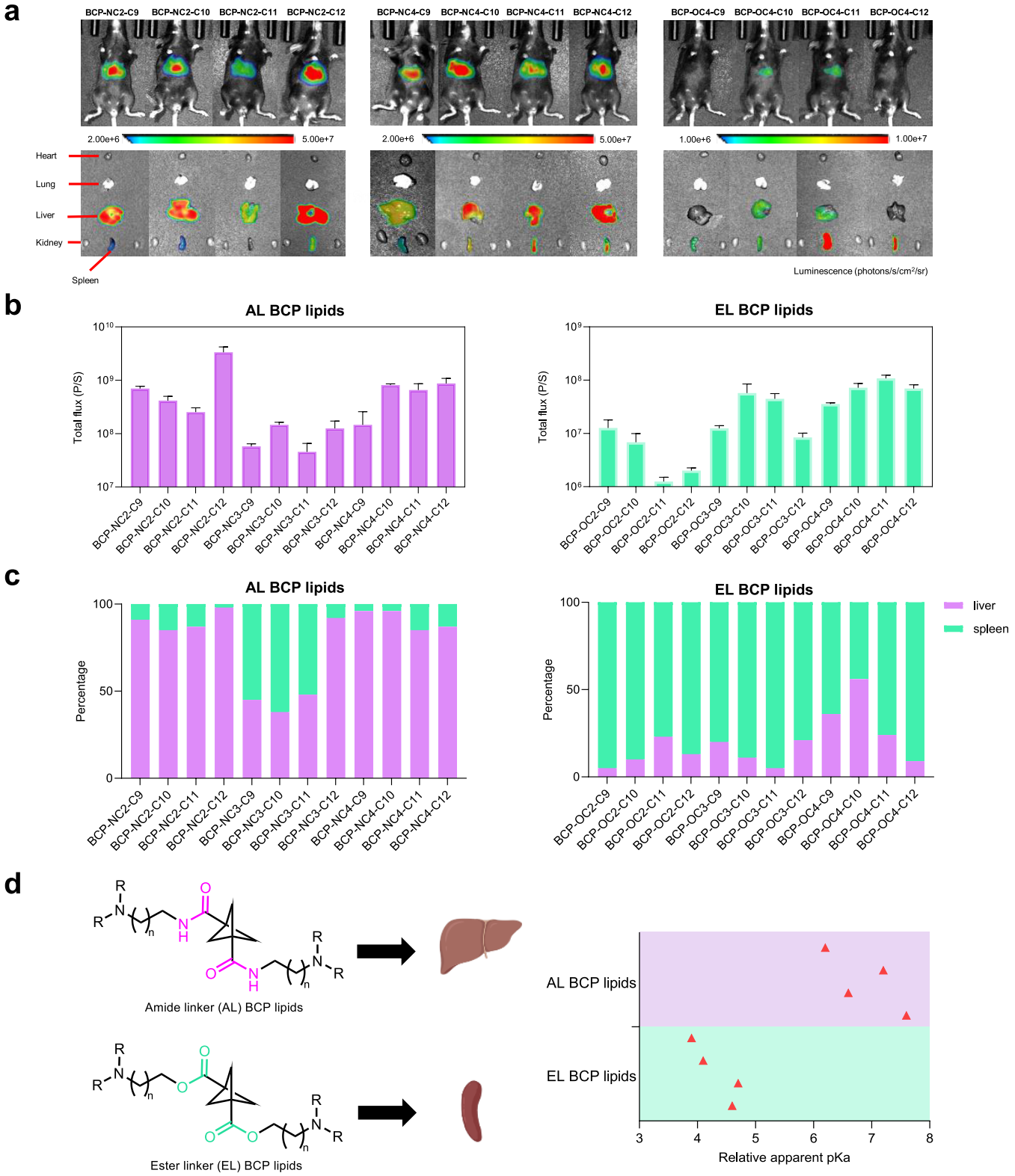

Figure 3. BCP LNPs effectively delivered mRNA *in vivo*. (a) Luciferase activity in C57BL/6 mice 6 h after IV injection of Luc mRNA LNPs (0.1 mg/kg, n = 3). Major organs from the top to the bottom: heart, lung, liver kidneys, and spleen. (b) Quantification of *in vivo* total luminescence in the liver and spleen of mice administered with AL and EL BCP LNPs (P/S, photons per second). (c) Percentage of luciferase expression in the liver and spleen. AL LNPs exhibited liver tropism, while EL LNPs displayed spleen tropism. (d) TNS assay curves for determining the apparent pK_a of LNPs based on NC4 linkers and OC4 linkers. Apparent pK_a was defined as the point at which 50% of the TNS fluorescence was achieved.

encapsulated in BCP LNPs IV, and whole-body bioluminescence images were recorded 6 h post injection. Based on the whole-body images (Figure S3), amide linker (AL) BCP lipids demonstrated a higher total luciferase activity (sum of liver and spleen signals) than ester linker (EL) BCP lipids (Figure 3a). Interestingly, the linker length of the ionizable lipids affected

https://doi.org/10.1021/jacs.4c13154
J. Am. Chem. Soc. 2024, 146, 34733−34742

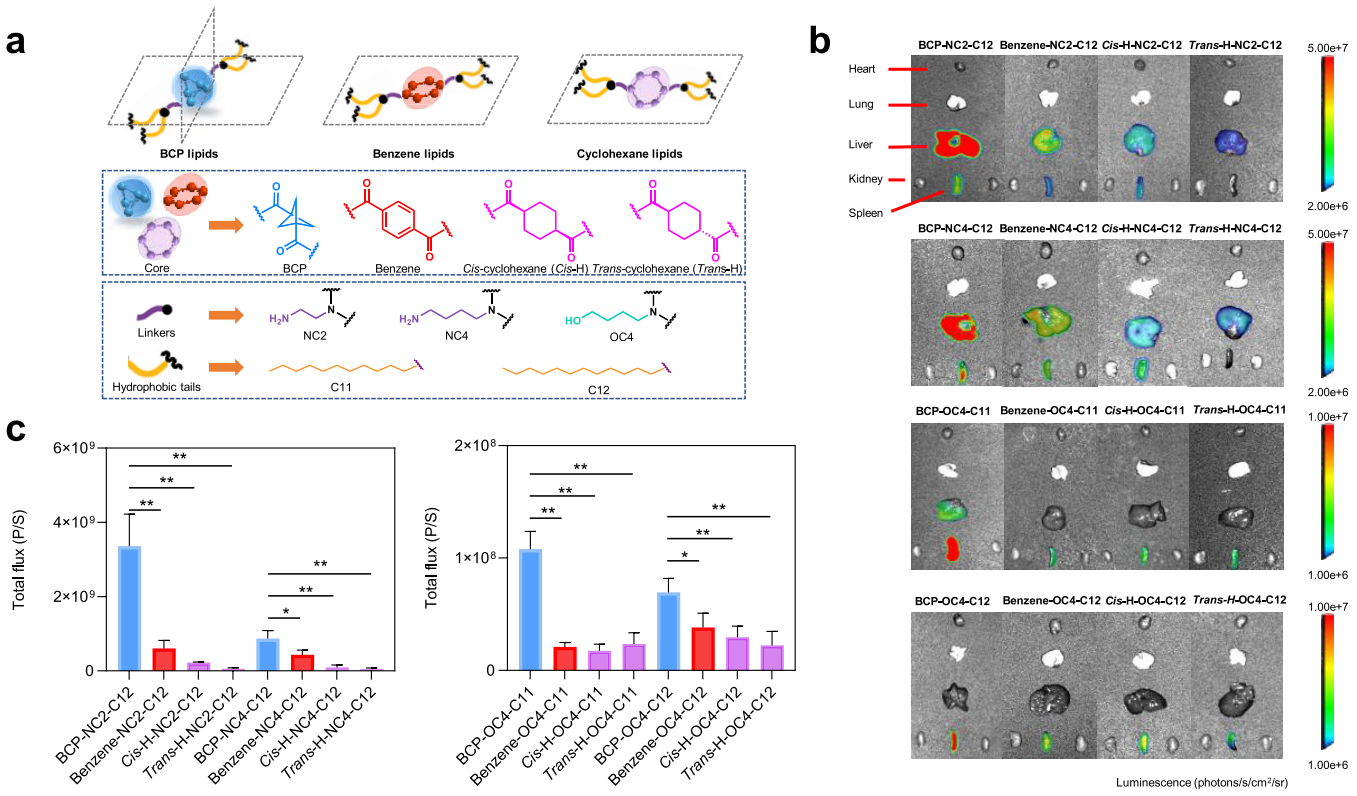

Figure 4. 3D BCP lipids outperformed analogous control lipids based on 2D benzene and cyclohexane cores. (a) BCP is a bioisosteric replacement for benzene and cyclohexane. To compare 3D and 2D analogues, a series of 3D BCP, 2D benzene, 2D *cis*-cyclohexane (*cis*-H), and 2D *trans*-cyclohexane (*trans*-H) core-based ionizable amino lipids were synthesized with NC2, NC4, and OC4 linkers as well as C11 and C12 hydrophobic tails. (b) Luciferase activity 6 h after IV administration of 3D and 2D-core LNPs formulated with AL BCP lipids (BCP-NC2-C12 and BCP-NC4-C12) and EL BCP lipids (BCP-OC4-C11 and BCP-OC4-C12) as well as their control lipids (2D benzene core and cyclohexane core-based lipids) at a dose of 0.1 mg/kg Luc mRNA. (c) Comparison of the total luciferase activity (P/S, photons per second). Statistical significance was analyzed by the *t* test (*$P < 0.05$; **$P < 0.01$; ***$P < 0.001$; ****$P < 0.0001$).

the mRNA delivery efficiencies (Figure 3b). For AL BCP lipids, 2-carbon (NC2) and 4-carbon (NC4) linkers showed a much higher transfection efficiency than 3-carbon (NC3) linkers, whereas for EL BCP lipids, 3-carbon (OC3) and 4-carbon (OC4) linkers resulted in better mRNA delivery than 2-carbon (OC2) linkers. The relationship between linker chemistry and mRNA transfection efficacy was consistent with the *in vitro* results. Meanwhile, BCP lipids containing ALs showed better delivery efficiency *in vivo* than ELs, which also matches the *in vitro* results (Figure 2c). Additionally, longer hydrophobic tails demonstrated greater transfection efficiency for AL BCP lipids. However, the optimized hydrophobic tails for EL BCP lipids were 10-carbon or 11-carbon, which showed higher protein activity. Overall, linker length and chemistry, as well as hydrophobic tail length, both played critical roles in determining the efficacy of ionizable lipids in LNPs. These factors may influence the polarity, solubility, and interaction of lipids with nucleic acids and cellular membranes, thereby affecting the delivery performance. Linker chemistry-dependent *in vivo* tropism preference was also observed. AL BCP LNPs exhibited mRNA-mediated Luc protein activity mainly in the liver, whereas EL BCP LNPs showed a spleen preference for mRNA transfection. Previous studies have indicated that mRNA delivery tropism correlates with apparent pK_a.[66] Liver delivery is associated with a pK_a between 6 and 7, while pK_a lower than 6 favors spleen delivery.[67] Therefore, we hypothesized that the tropism preference between AL BCP lipids and EL BCP lipids may be due to the different pK_a values of LNPs affected by the ALs and ELs. To test this, we tested the pK_a values of LNPs formulated with BCP lipids using the 6-*p*-toluidinylnaphthalene-2-sulfonate (TNS) assay.[67] Indeed, NC4-based BCP LNPs possessed pK_a values from 6 to 8, while OC4-based BCP LNPs had pK_a values around 4−5 (Figure 3d). This finding agrees with the established precedent for organ tropism. The differing pK_a between AL and EL lipids may be related to their differing electron-withdrawing and hydrogen-bonding properties. Among all BCP lipids, BCP-NC2-C12 and BCP-OC4-C11 lipids demonstrated the highest mRNA delivery efficacy in their respective AL and EL lipid groups. BCP-NC2-C12 LNPs delivered mRNA 25-fold more effectively to the liver *in vivo* than benchmark DLin-MC3-DMA LNPs at the same dose (Figure S4). Since DLin-MC3-DMA LNPs are used clinically for liver therapy, these results suggest promise for BCP LNPs.

3D BCP LNPs Are More Efficacious than 2D Benzene and Cyclohexane Analogues. In small-molecule drugs, BCP serves as a valuable bioisostere for benzene. To examine whether the 3D nature of BCP lipids would improve mRNA delivery over the 2D benzene equivalents, we designed and synthesized a series of control lipids. In addition to benzene, we also explored *cis*- and *trans*-cyclohexane to further examine the potential effects of aromaticity and stereochemistry. We synthetically replaced the BCP cores of BCP-NC2-C12, BCP-NC4-C12, BCP-OC4-C11, and BCP-OC4-C12 with the 2D cores of benzene, *cis*-cyclohexane (*cis*-H), and *trans*-cyclohexane (*trans*-H) (Figures S5 and 4a). The synthetic routes

https://doi.org/10.1021/jacs.4c13154
J. Am. Chem. Soc. 2024, 146, 34733−34742

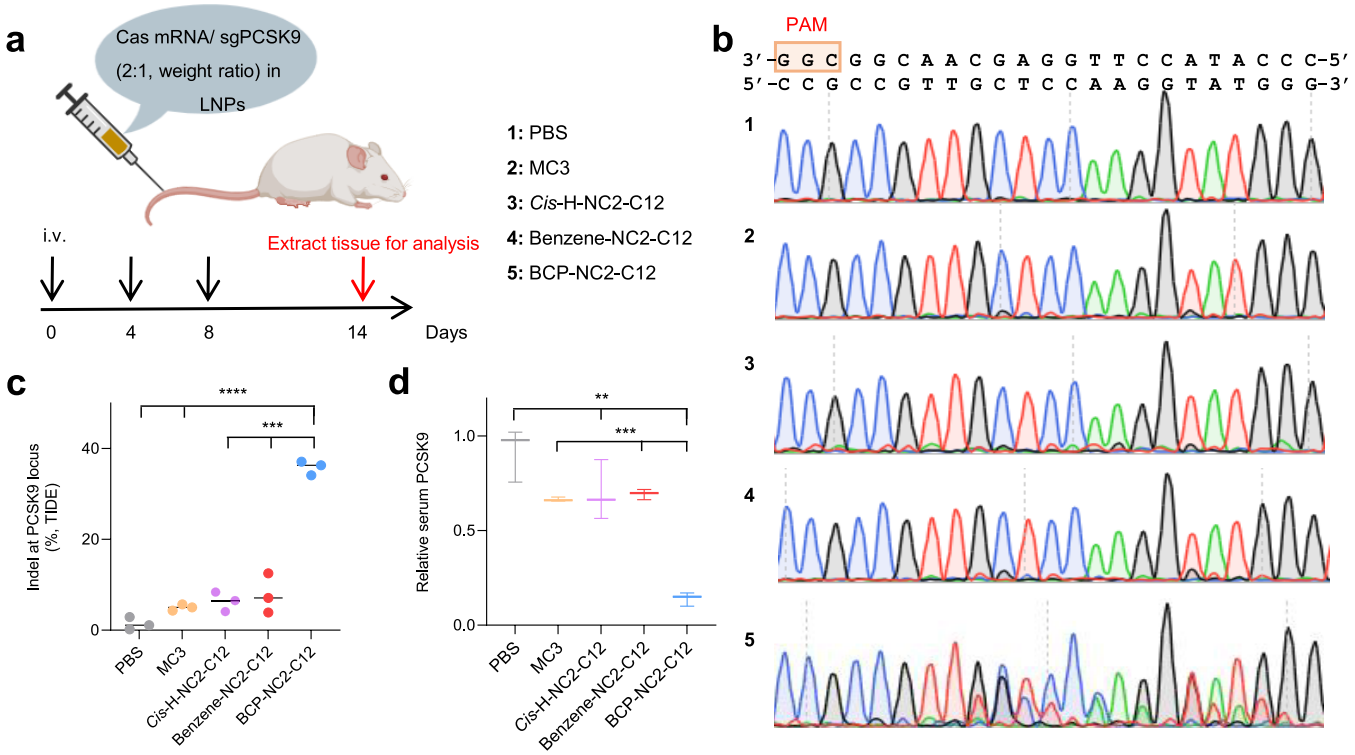

Figure 5. BCP-NC2-C12 LNPs more effectively codelivered Cas9 mRNA and sgPCSK9 to C57BL/6 mice than BCP-NC2-C12, benzene-NC2-C12, HC-NC2-C12, and MC3 reference LNPs. (a) C57BL/6 mice were treated with three IV injections (days 0, 4, 8) (n = 3, biologically independent animals). On day 14, liver and serum samples were collected for analysis. (b) Comparison of Sanger sequencing among PBS, MC3, *cis*-H-NC2-C12, benzene-NC2-C12, and BCP-NC2-C12 groups. The cut is expected to occur upstream of the protospacer adjacent motif, 5′ to 3′ of sg*PCSK9*: CGG. (c) *Pcsk9* locus of liver tissue quantified using TIDE analysis. (d) BCP-NC2-C12 LNPs resulted in ∼90% PCSK9 protein reduction in the serum (ELISA). A t test was used to determine the significance of the comparisons of data indicated in c and d (*P < 0.05; **P < 0.01; ***P < 0.001; ****P < 0.0001).

remained the same as those of BCP lipids (Scheme S14). The purified lipids were self-assembled into LNPs containing Luc mRNA with all other variables being kept constant other than the ionizable amino lipid (ionizable amino lipid/DOPE/cholesterol/PEG2k-DMG = 23.8/23.8/47.6/4.8, molar percentages %). The resulting LNPs demonstrated similar hydrodynamic diameters and PDIs (Figure S6). Control 2D-core LNPs were less efficient at delivering mRNA *in vitro* compared to BCP LNPs (Figure S7a). We then compared *in vivo* mRNA delivery efficacy with that of BCP counterparts. Both AL and EL BCP LNPs exhibited significantly higher luciferase expression than those formulated with analogous 2D-core benzene, *cis*-cyclohexane, and *trans*-cyclohexane lipids (Figure 4b,c). These results highlight the unique 3D structured BCP nature that boosts mRNA delivery. Encouragingly, the same liver and spleen tropism profiles were observed for the control lipids as for the BCP lipids (Figure S7b). This result suggests that the control analogues are suitable comparators and establish differences in delivery potency corresponding to 3D and 2D architectures. Next, cryo-electron microscopy (EM) was used to analyze the structure of BCP-NC2-C12, benzene-NC2-C12, and *Cis*-H-NC2-C12 LNPs (Figure S14). All three LNPs adopted a bilayer structure. BCP-NC2-C12-based LNPs appear to display a morphology resembling the bicontinuous cubic phase (QII).[68] Future investigations will be required to more definitively connect the irregular nanostructure surface to the potential improvement of the LNP-endosome membrane fusion.

BCP LNPs Mediate Efficient *Pcsk9* Knockout in the Liver. To evaluate the suitability of BCP LNPs for therapeutic applications, we employed CRISPR/Cas gene editing technology to disrupt the *Psck9* gene in a proof-of-concept study. *Pcsk9* is an attractive therapeutic target in the treatment of familial hypercholesterolemia and atherosclerotic cardiovascular disease.[8,69,70] We codelivered Cas9 encoding mRNA and a single guide RNA targeting the *Pcsk9* gene using BCP LNPs, control LNPs, and a benchmark LNP (Figure 5a). BCP-NC2-C12 LNPs were selected based on their superior performance in Luc mRNA delivery. We investigated gene knockout and phenotypic changes in C57BL/6 mice. Cas9 mRNA and sgPCSK9 were copackaged in BCP-NC2-C12, benzene-NC2-C12, *cis*-H-NC2-C12, and DLin-MC3-DMA LNPs. All LNPs were uniform in size (∼80 nm) with a low PDI and high RNA encapsulation efficiencies (Figure S9). C57BL/6 mice were administered IV with different LNP formulations containing the same dosage of total RNA (2.5 mg/kg) on days 0, 4, and 8 (Figure 5a). On day 14, liver tissue and serum samples were collected from mice for analysis. LNPs formulated with 3D BCP lipid (BCP-NC2-C12) induced significant insertions and deletions (indels) at the *Pcsk9* locus (∼36% confirmed using TIDE, Figure 5b,c), leading to a ∼90% reduction in the PCSK9 protein level in the blood (Figure 5d) and in the liver (Figure S10). In contrast, LNPs containing control lipids (MC3, benzene-NC2-C12, and *cis*-H-NC2-C12) enabled only 5−8% indels at the *Pcsk9* locus, resulting in a low reduction in PCSK9 protein levels. We next performed histology to examine liver tissues from the various treatment groups with

https://doi.org/10.1021/jacs.4c13154
J. Am. Chem. Soc. 2024, 146, 34733−34742

hematoxylin-eosin (H&E) staining (Figure S11). No differences were observed between the PBS and LNP-treated animals, indicating that all of the tested LNPs showed a favorable safety profile. Overall, these findings highlight that BCP-NC2-C12 LNPs outperformed all controls and benchmark MC3, indicating that 3D core BCP-NC2-C12 BCP LNPs hold promise for therapeutic mRNA and genome editing applications.

CONCLUSIONS

Inspired by the success of highly strained bioisosteres in small-molecule drug design, we incorporated a 3D BCP structure into an ionizable amino lipid design. Through modular synthesis, we created a library of BCP lipids and thoroughly studied SARs for mRNA delivery *in vitro* and *in vivo*. 3D BCP lipids significantly outperformed their 2D-core counterparts across all assays, indicating the unique efficacy of 3D designs. The highly strained BCP structure resulted in 25-fold superior mRNA delivery efficacy compared to a clinically used MC3 LNP benchmark in the liver. *In vivo*, tissue tropism was controlled through the modulation of ALs and ELs. Lead 3D BCP LNPs demonstrated highly efficient CRISPR/Cas gene editing *in vivo*, outperforming MC3 LNPs 7.2-fold. BCP-NC2-C12 LNPs were well-tolerated, highlighting their potential clinical applicability. We envision that this work can open new avenues for ionizable lipid design and enable enhanced efficiency for broad medical applications.

ASSOCIATED CONTENT

Supporting Information

The Supporting Information is available free of charge at https://pubs.acs.org/doi/10.1021/jacs.4c13154.

Materials, experimental procedures, synthesis procedures, preparation and characterization of LNPs, statistical analyses, supporting schemes and figures, and ^{1}H NMR and ^{13}C NMR spectra (PDF)

AUTHOR INFORMATION

Corresponding Authors

Tian Qin − *Department of Biochemistry, The University of Texas Southwestern Medical Center, Dallas, Texas 75390, United States;* orcid.org/0000-0001-7225-3224; Email: tian.qin@utsouthwestern.edu

Daniel J. Siegwart − *Department of Biomedical Engineering, Department of Biochemistry, Simmons Comprehensive Cancer Center, Program in Genetic Drug Engineering, The University of Texas Southwestern Medical Center, Dallas, Texas 75390, United States;* orcid.org/0000-0003-3823-1931; Email: daniel.siegwart@utsouthwestern.edu

Authors

Shiying Wu − *Department of Biomedical Engineering, Department of Biochemistry, Simmons Comprehensive Cancer Center, Program in Genetic Drug Engineering, The University of Texas Southwestern Medical Center, Dallas, Texas 75390, United States;* orcid.org/0000-0002-6902-9544

Yangyang Yang − *Department of Biomedical Engineering, Department of Biochemistry, Simmons Comprehensive Cancer Center, Program in Genetic Drug Engineering, The University of Texas Southwestern Medical Center, Dallas, Texas 75390, United States*

Xizhen Lian − *Department of Biomedical Engineering, Department of Biochemistry, Simmons Comprehensive Cancer Center, Program in Genetic Drug Engineering, The University of Texas Southwestern Medical Center, Dallas, Texas 75390, United States*

Fangyu Zhang − *Department of Biomedical Engineering, Department of Biochemistry, Simmons Comprehensive Cancer Center, Program in Genetic Drug Engineering, The University of Texas Southwestern Medical Center, Dallas, Texas 75390, United States;* orcid.org/0000-0002-6522-5230

Chao Hu − *Department of Biochemistry, The University of Texas Southwestern Medical Center, Dallas, Texas 75390, United States*

Jet Tsien − *Department of Biochemistry, The University of Texas Southwestern Medical Center, Dallas, Texas 75390, United States;* orcid.org/0000-0002-2052-8051

Zexiang Chen − *Department of Biomedical Engineering, Department of Biochemistry, Simmons Comprehensive Cancer Center, Program in Genetic Drug Engineering, The University of Texas Southwestern Medical Center, Dallas, Texas 75390, United States*

Yehui Sun − *Department of Biomedical Engineering, Department of Biochemistry, Simmons Comprehensive Cancer Center, Program in Genetic Drug Engineering, The University of Texas Southwestern Medical Center, Dallas, Texas 75390, United States;* orcid.org/0000-0003-0215-6095

Amogh Vaidya − *Department of Biomedical Engineering, Department of Biochemistry, Simmons Comprehensive Cancer Center, Program in Genetic Drug Engineering, The University of Texas Southwestern Medical Center, Dallas, Texas 75390, United States*

Minjeong Kim − *Department of Biomedical Engineering, Department of Biochemistry, Simmons Comprehensive Cancer Center, Program in Genetic Drug Engineering, The University of Texas Southwestern Medical Center, Dallas, Texas 75390, United States*

Yun-Chieh Sung − *Department of Biomedical Engineering, Department of Biochemistry, Simmons Comprehensive Cancer Center, Program in Genetic Drug Engineering, The University of Texas Southwestern Medical Center, Dallas, Texas 75390, United States*

Yufen Xiao − *Department of Biomedical Engineering, Department of Biochemistry, Simmons Comprehensive Cancer Center, Program in Genetic Drug Engineering, The University of Texas Southwestern Medical Center, Dallas, Texas 75390, United States;* orcid.org/0000-0002-5604-7479

Xiaoyan Bian − *Department of Biomedical Engineering, Department of Biochemistry, Simmons Comprehensive Cancer Center, Program in Genetic Drug Engineering, The University of Texas Southwestern Medical Center, Dallas, Texas 75390, United States*

Xu Wang − *Department of Biomedical Engineering, Department of Biochemistry, Simmons Comprehensive Cancer Center, Program in Genetic Drug Engineering, The University of Texas Southwestern Medical Center, Dallas, Texas 75390, United States;* orcid.org/0000-0002-8925-5645

Zeru Tian − *Department of Biomedical Engineering, Department of Biochemistry, Simmons Comprehensive Cancer Center, Program in Genetic Drug Engineering, The*

https://doi.org/10.1021/jacs.4c13154
J. Am. Chem. Soc. 2024, 146, 34733−34742

University of Texas Southwestern Medical Center, Dallas, Texas 75390, United States

Erick Guerrero − *Department of Biomedical Engineering, Department of Biochemistry, Simmons Comprehensive Cancer Center, Program in Genetic Drug Engineering, The University of Texas Southwestern Medical Center, Dallas, Texas 75390, United States*

Joshua Robinson − *Department of Biomedical Engineering, Department of Biochemistry, Simmons Comprehensive Cancer Center, Program in Genetic Drug Engineering, The University of Texas Southwestern Medical Center, Dallas, Texas 75390, United States*

Pratima Basak − *Department of Biomedical Engineering, Department of Biochemistry, Simmons Comprehensive Cancer Center, Program in Genetic Drug Engineering, The University of Texas Southwestern Medical Center, Dallas, Texas 75390, United States*

Complete contact information is available at: https://pubs.acs.org/10.1021/jacs.4c13154

Notes

The authors declare the following competing financial interest(s): DJS is a co-founder of ReCode Therapeutics, Signify Bio, and Jumble Therapeutics.

■ ACKNOWLEDGMENTS

D.J.S. acknowledges financial support from the National Institutes of Health (NIH), the National Institute of Biomedical Imaging and Bioengineering (NIBIB) (R01 5R01EB025192-06), the National Cancer Institute (R01 CA269787-01), and the Welch Foundation (I-2123-20220031). T.Q. acknowledges support from the National Science Foundation (CHE-2143925) and the Welch Foundation (I-2155-20230405). The authors thank Feng Lin (UTSW) for assistance with NMR spectroscopy and Hamid Baniasadi (UTSW) for mass spectrometry analysis. The authors also acknowledge support from the UTSW Small Animal Imaging Resource (NCI P30CA142543), the UTSW Proteomics Core (NIH R01 CA248736), and the Cryo-Electron Microscopy Facility (CEMF) (CPRIT RP170644 and RP220582).

■ REFERENCES

(1) Barbier, A. J.; Jiang, A. Y.; Zhang, P.; Wooster, R.; Anderson, D. G. The clinical progress of mRNA vaccines and immunotherapies. *Nat. Biotechnol.* **2022**, *40* (6), 840−854.

(2) Chen, Z.; Tian, Y.; Yang, J.; Wu, F.; Liu, S.; Cao, W.; Xu, W.; Hu, T.; Siegwart, D. J.; Xiong, H. Modular design of biodegradable ionizable lipids for improved mRNA delivery and precise cancer metastasis delineation in vivo. *J. Am. Chem. Soc.* **2023**, *145* (44), 24302−24314.

(3) Cheng, Q.; Wei, T.; Farbiak, L.; Johnson, L. T.; Dilliard, S. A.; Siegwart, D. J. Selective organ targeting (SORT) nanoparticles for tissue-specific mRNA delivery and CRISPR−Cas gene editing. *Nat. Nanotechnol.* **2020**, *15* (4), 313−320.

(4) Hajj, K. A.; Whitehead, K. A. Tools for translation: Non-viral materials for therapeutic mRNA delivery. *Nat. Rev. Mater.* **2017**, *2* (10), 17056.

(5) Li, D.; Liu, C.; Li, Y.; Tenchov, R.; Sasso, J. M.; Zhang, D.; Li, D.; Zou, L.; Wang, X.; Zhou, Q. Messenger RNA-based therapeutics and vaccines: What's beyond COVID-19? *ACS Pharmacol. Transl. Sci.* **2023**, *6* (7), 943−969.

(6) Lian, X.; Chatterjee, S.; Sun, Y.; Dilliard, S. A.; Moore, S.; Xiao, Y.; Bian, X.; Yamada, K.; Sung, Y.-C.; Levine, R. M.; Mayberry, K.; John, S.; Liu, X.; Smith, C.; Johnson, L. T.; Wang, X.; Zhang, C. C.; Liu, D. R.; Newby, G. A.; Weiss, M. J.; Yen, J. S.; Siegwart, D. J. Bone-marrow-homing lipid nanoparticles for genome editing in diseased and malignant haematopoietic stem cells. *Nat. Nanotechnol.* **2024**, *19* (9), 1409−1417.

(7) Liu, S.; Cheng, Q.; Wei, T.; Yu, X.; Johnson, L. T.; Farbiak, L.; Siegwart, D. J. Membrane-destabilizing ionizable phospholipids for organ-selective mRNA delivery and CRISPR-Cas gene editing. *Nat. Mater.* **2021**, *20* (5), 701−710.

(8) Musunuru, K.; Chadwick, A. C.; Mizoguchi, T.; Garcia, S. P.; DeNizio, J. E.; Reiss, C. W.; Wang, K.; Iyer, S.; Dutta, C.; Clendaniel, V.; Amaonye, M.; Beach, A.; Berth, K.; Biswas, S.; Braun, M. C.; Chen, H.-M.; Colace, T. V.; Ganey, J. D.; Gangopadhyay, S. A.; Garrity, R.; Kasiewicz, L. N.; Lavoie, J.; Madsen, J. A.; Matsumoto, Y.; Mazzola, A. M.; Nasrullah, Y. S.; Nneji, J.; Ren, H.; Sanjeev, A.; Shay, M.; Stahley, M. R.; Fan, S. H. Y.; Tam, Y. K.; Gaudelli, N. M.; Ciaramella, G.; Stolz, L. E.; Malyala, P.; Cheng, C. J.; Rajeev, K. G.; Rohde, E.; Bellinger, A. M.; Kathiresan, S. In vivo CRISPR base editing of PCSK9 durably lowers cholesterol in primates. *Nature* **2021**, *593* (7859), 429−434.

(9) Pardi, N.; Hogan, M. J.; Porter, F. W.; Weissman, D. mRNA vaccines — A new era in vaccinology. *Nat. Rev. Drug Discovery* **2018**, *17* (4), 261−279.

(10) Sahin, U.; Karikó, K.; Türeci, Ö. mRNA-based therapeutics — Developing a new class of drugs. *Nat. Rev. Drug Discovery* **2014**, *13* (10), 759−780.

(11) Sun, Y.; Chatterjee, S.; Lian, X.; Traylor, Z.; Sattiraju, S. R.; Xiao, Y.; Dilliard, S. A.; Sung, Y.-C.; Kim, M.; Lee, S. M.; Moore, S.; Wang, X.; Zhang, D.; Wu, S.; Basak, P.; Wang, J.; Liu, J.; Mann, R. J.; LePage, D. F.; Jiang, W.; Abid, S.; Hennig, M.; Martinez, A.; Wustman, B. A.; Lockhart, D. J.; Jain, R.; Conlon, R. A.; Drumm, M. L.; Hodges, C. A.; Siegwart, D. J. In vivo editing of lung stem cells for durable gene correction in mice. *Science* **2024**, *384* (6701), 1196−1202.

(12) Wang, H. X.; Li, M.; Lee, C. M.; Chakraborty, S.; Kim, H. W.; Bao, G.; Leong, K. W. CRISPR/Cas9-based genome editing for disease modeling and therapy: Challenges and opportunities for nonviral delivery. *Chem. Rev.* **2017**, *117* (15), 9874−9906.

(13) Wei, T.; Cheng, Q.; Farbiak, L.; Anderson, D. G.; Langer, R.; Siegwart, D. J. Delivery of tissue-targeted scalpels: Opportunities and challenges for in vivo CRISPR/Cas-based genome editing. *ACS Nano* **2020**, *14* (8), 9243−9262.

(14) Baden, L. R.; Sahly, H. M. E.; Essink, B.; Kotloff, K.; Frey, S.; Novak, R.; Diemert, D.; Spector, S. A.; Rouphael, N.; Creech, C. B.; McGettigan, J.; Khetan, S.; Segall, N.; Solis, J.; Brosz, A.; Fierro, C.; Schwartz, H.; Neuzil, K.; Corey, L.; Gilbert, P.; Janes, H.; Follmann, D.; Marovich, M.; Mascola, J.; Polakowski, L.; Ledgerwood, J.; Graham, B. S.; Bennett, H.; Pajon, R.; Knightly, C.; Leav, B.; Deng, W.; Zhou, H.; Han, S.; Ivarsson, M.; Miller, J.; Zaks, T. Efficacy and Safety of the mRNA-1273 SARS-CoV-2 Vaccine. *N. Engl. J. Med.* **2021**, *384* (5), 403−416.

(15) Polack, F. P.; Thomas, S. J.; Kitchin, N.; Absalon, J.; Gurtman, A.; Lockhart, S.; Perez, J. L.; Marc, G. P.; Moreira, E. D.; Zerbini, C.; Bailey, R.; Swanson, K. A.; Roychoudhury, S.; Koury, K.; Li, P.; Kalina, W. V.; Cooper, D.; Frenck, R. W.; Hammitt, L. L.; Türeci, Ö.; Nell, H.; Schaefer, A.; Ünal, S.; Tresnan, D. B.; Mather, S.; Dormitzer, P. R.; Şahin, U.; Jansen, K. U.; Gruber, W. C. Safety and efficacy of the BNT162b2 mRNA COVID-19 vaccine. *N. Engl. J. Med.* **2020**, *383* (27), 2603−2615.

(16) Benner, N. L.; McClellan, R. L.; Turlington, C. R.; Haabeth, O. A. W.; Waymouth, R. M.; Wender, P. A. Oligo(serine ester) charge-altering releasable transporters: Organocatalytic ring-opening polymerization and their use for in vitro and in vivo mRNA delivery. *J. Am. Chem. Soc.* **2019**, *141* (21), 8416−8421.

(17) Chen, Q.; Wang, X.; Zhang, Y.; Tian, M.; Duan, J.; Zhang, Y.; Yin, H. Minimizing the ratio of ionizable lipid in lipid nanoparticles for in vivo base editing. *Natl. Sci. Rev.* **2024**, *11* (6), nwae135.

(18) Dehghani-Ghahnaviyeh, S.; Smith, M.; Xia, Y.; Dousis, A.; Grossfield, A.; Sur, S. Ionizable amino lipids distribution and effects

on DSPC/cholesterol membranes: Implications for lipid nanoparticle structure. *J. Phys. Chem. B* **2023**, *127* (31), 6928−6939.
(19) Han, X.; Zhang, H.; Butowska, K.; Swingle, K. L.; Alameh, M.-G.; Weissman, D.; Mitchell, M. J. An ionizable lipid toolbox for RNA delivery. *Nat. Commun.* **2021**, *12* (1), 7233.
(20) Hou, X.; Zaks, T.; Langer, R.; Dong, Y. Lipid nanoparticles for mRNA delivery. *Nat. Rev. Mater.* **2021**, *6* (12), 1078−1094.
(21) Liu, S.; Wang, X.; Yu, X.; Cheng, Q.; Johnson, L. T.; Chatterjee, S.; Zhang, D.; Lee, S. M.; Sun, Y.; Lin, T.-C.; Liu, J. L.; Siegwart, D. J. Zwitterionic phospholipidation of cationic polymers facilitates systemic mRNA delivery to spleen and lymph nodes. *J. Am. Chem. Soc.* **2021**, *143* (50), 21321−21330.
(22) Sun, D.; Lu, Z. R. Structure and function of cationic and ionizable lipids for nucleic acid delivery. *Pharm. Res.* **2023**, *40* (1), 27−46.
(23) Xue, L.; Gong, N.; Shepherd, S. J.; Xiong, X.; Liao, X.; Han, X.; Zhao, G.; Song, C.; Huang, X.; Zhang, H.; Padilla, M. S.; Qin, J.; Shi, Y.; Alameh, M.-G.; Pochan, D. J.; Wang, K.; Long, F.; Weissman, D.; Mitchell, M. J. Rational design of bisphosphonate lipid-like materials for mRNA delivery to the bone microenvironment. *J. Am. Chem. Soc.* **2022**, *144* (22), 9926−9937.
(24) Zhang, D.; Atochina-Vasserman, E. N.; Maurya, D. S.; Huang, N.; Xiao, Q.; Ona, N.; Liu, M.; Shahnawaz, H.; Ni, H.; Kim, K.; Billingsley, M. M.; Pochan, D. J.; Mitchell, M. J.; Weissman, D.; Percec, V. One-component multifunctional sequence-defined ionizable amphiphilic Janus dendrimer delivery systems for mRNA. *J. Am. Chem. Soc.* **2021**, *143* (31), 12315−12327.
(25) Zhang, Y.; Sun, C.; Wang, C.; Jankovic, K. E.; Dong, Y. Lipids and lipid derivatives for RNA delivery. *Chem. Rev.* **2021**, *121* (20), 12181−12277.
(26) Zhao, X.; Chen, J.; Qiu, M.; Li, Y.; Glass, Z.; Xu, Q. Imidazole-based synthetic lipidoids for in vivo mRNA delivery into primary T lymphocytes. *Angew. Chem., Int. Ed.* **2020**, *59* (45), 20083−20089.
(27) Dilliard, S. A.; Siegwart, D. J. Passive, active and endogenous organ-targeted lipid and polymer nanoparticles for delivery of genetic drugs. *Nat. Rev. Mater.* **2023**, *8* (4), 282−300.
(28) Li, B.; Raji, I. O.; Gordon, A. G. R.; Sun, L.; Raimondo, T. M.; Oladimeji, F. A.; Jiang, A. Y.; Varley, A.; Langer, R. S.; Anderson, D. G. Accelerating ionizable lipid discovery for mRNA delivery using machine learning and combinatorial chemistry. *Nat. Mater.* **2024**, *23* (7), 1002−1008.
(29) Ai, H.; Wu, D.; Zhou, H.; Xu, J.; Gu, Q. dMXP: A de novo small-molecule 3D structure predictor with graph attention networks. *J. Chem. Inf. Model.* **2024**, *64* (9), 3744−3755.
(30) Levin, M. D.; Kaszynski, P.; Michl, J. Bicyclo[1.1.1]pentanes, [n]staffanes, [1.1.1]propellanes, and tricyclo[2.1.0.02,5]pentanes. *Chem. Rev.* **2000**, *100* (1), 169−234.
(31) Lovering, F.; Bikker, J.; Humblet, C. Escape from Flatland: Increasing saturation as an approach to improving clinical success. *J. Med. Chem.* **2009**, *52* (21), 6752−6756.
(32) Prosser, K. E.; Stokes, R. W.; Cohen, S. M. Evaluation of 3-dimensionality in approved and experimental drug space. *ACS Med. Chem. Lett.* **2020**, *11* (6), 1292−1298.
(33) Reekie, T. A.; Williams, C. M.; Rendina, L. M.; Kassiou, M. Cubanes in medicinal chemistry. *J. Med. Chem.* **2019**, *62* (3), 1078−1095.
(34) Tse, E. G.; Houston, S. D.; Williams, C. M.; Savage, G. P.; Rendina, L. M.; Hallyburton, I.; Anderson, M.; Sharma, R.; Walker, G. S.; Obach, R. S.; Todd, M. H. Nonclassical phenyl bioisosteres as effective replacements in a series of novel open-source antimalarials. *J. Med. Chem.* **2020**, *63* (20), 11585−11601.
(35) Zhung, W.; Kim, H.; Kim, W. Y. 3D molecular generative framework for interaction-guided drug design. *Nat. Commun.* **2024**, *15* (1), 2688.
(36) Brown, D. G.; Gagnon, M. M.; Boström, J. Understanding our love affair with p-chlorophenyl: Present day implications from historical biases of reagent selection. *J. Med. Chem.* **2015**, *58* (5), 2390−2405.
(37) Hansch, C.; Leo, A.; Unger, S. H.; Kim, K. H.; Nikaitani, D.; Lien, E. J. Aromatic substituent constants for structure-activity correlations. *J. Med. Chem.* **1973**, *16* (11), 1207−1216.
(38) Salonen, L. M.; Ellermann, M.; Diederich, F. Aromatic rings in chemical and biological recognition: Energetics and structures. *Angew. Chem., Int. Ed.* **2011**, *50* (21), 4808−4842.
(39) Shearer, J.; Castro, J. L.; Lawson, A. D. G.; MacCoss, M.; Taylor, R. D. Rings in clinical trials and drugs: Present and future. *J. Med. Chem.* **2022**, *65* (13), 8699−8712.
(40) Taylor, R. D.; MacCoss, M.; Lawson, A. D. Rings in drugs: Miniperspective. *J. Med. Chem.* **2014**, *57* (14), 5845−5859.
(41) Nilova, A.; Campeau, L.-C.; Sherer, E. C.; Stuart, D. R. Analysis of benzenoid substitution patterns in small molecule active pharmaceutical ingredients: Miniperspective. *J. Med. Chem.* **2020**, *63* (22), 13389−13396.
(42) Subbaiah, M. A. M.; Meanwell, N. A. Bioisosteres of the phenyl ring: Recent strategic applications in lead optimization and drug design. *J. Med. Chem.* **2021**, *64* (19), 14046−14128.
(43) Young, R. J.; Green, D. V. S.; Luscombe, C. N.; Hill, A. P. Getting physical in drug discovery II: the impact of chromatographic hydrophobicity measurements and aromaticity. *Drug Discovery Today* **2011**, *16* (17), 822−830.
(44) Ritchie, T. J.; Macdonald, S. J. F. The impact of aromatic ring count on compound developability−are too many aromatic rings a liability in drug design? *Drug Discovery Today* **2009**, *14* (21), 1011−1020.
(45) Tsien, J.; Hu, C.; Merchant, R. R.; Qin, T. Three-dimensional saturated C(sp3)-rich bioisosteres for benzene. *Nat. Rev. Chem.* **2024**, *8* (8), 605−627.
(46) Stepan, A. F.; Subramanyam, C.; Efremov, I. V.; Dutra, J. K.; O'Sullivan, T. J.; DiRico, K. J.; McDonald, W. S.; Won, A.; Dorff, P. H.; Nolan, C. E.; Becker, S. L.; Pustilnik, L. R.; Riddell, D. R.; Kauffman, G. W.; Kormos, B. L.; Zhang, L.; Lu, Y.; Capetta, S. H.; Green, M. E.; Karki, K.; Sibley, E.; Atchison, K. P.; Hallgren, A. J.; Oborski, C. E.; Robshaw, A. E.; Sneed, B.; O'Donnell, C. J. Application of the bicyclo[1.1.1]pentane motif as a nonclassical phenyl ring bioisostere in the design of a potent and orally active γ-secretase inhibitor. *J. Med. Chem.* **2012**, *55* (7), 3414−3424.
(47) Measom, N. D.; Down, K. D.; Hirst, D. J.; Jamieson, C.; Manas, E. S.; Patel, V. K.; Somers, D. O. Investigation of a bicyclo[1.1.1]-pentane as a phenyl replacement within an LpPLA2 inhibitor. *ACS Med. Chem. Lett.* **2017**, *8* (1), 43−48.
(48) Gianatassio, R.; Lopchuk, J. M.; Wang, J.; Pan, C.-M.; Malins, L. R.; Prieto, L.; Brandt, T. A.; Collins, M. R.; Gallego, G. M.; Sach, N. W. Strain-release amination. *Science* **2016**, *351* (6270), 241−246.
(49) Zhao, J. X.; Chang, Y. X.; He, C.; Burke, B. J.; Collins, M. R.; Del Bel, M.; Elleraas, J.; Gallego, G. M.; Montgomery, T. P.; Mousseau, J. J.; Nair, S. K.; Perry, M. A.; Spangler, J. E.; Vantourout, J. C.; Baran, P. S. 1,2-Difunctionalized bicyclo[1.1.1]pentanes: Long-sought-after mimetics for ortho/meta-substituted arenes. *Proc. Natl. Acad. Sci. U. S. A.* **2021**, *118* (28), No. e2108881118.
(50) Zhang, X.; Smith, R. T.; Le, C.; McCarver, S. J.; Shireman, B. T.; Carruthers, N. I.; MacMillan, D. W. C. Copper-mediated synthesis of drug-like bicyclopentanes. *Nature* **2020**, *580* (7802), 220−226.
(51) Yang, Y.; Tsien, J.; Ben David, A.; Hughes, J. M. E.; Merchant, R. R.; Qin, T. Practical and modular construction of C(sp3)-rich alkyl boron compounds. *J. Am. Chem. Soc.* **2021**, *143* (1), 471−480.
(52) Yang, Y.; Tsien, J.; Hughes, J. M. E.; Peters, B. K.; Merchant, R. R.; Qin, T. An intramolecular coupling approach to alkyl bioisosteres for the synthesis of multisubstituted bicycloalkyl boronates. *Nat. Chem.* **2021**, *13* (10), 950−955.
(53) Wright, B. A.; Matviitsuk, A.; Black, M. J.; García-Reynaga, P.; Hanna, L. E.; Herrmann, A. T.; Ameriks, M. K.; Sarpong, R.; Lebold, T. P. Skeletal editing approach to bridge-functionalized bicyclo [1.1.1] pentanes from azabicyclo [2.1. 1] hexanes. *J. Am. Chem. Soc.* **2023**, *145* (20), 10960−10966.
(54) Zhou, M.; Tsien, J.; Dykstra, R.; Hughes, J. M. E.; Peters, B. K.; Merchant, R. R.; Gutierrez, O.; Qin, T. Alkyl sulfinates as cross-

coupling partners for programmable and stereospecific installation of C(sp3) bioisosteres. *Nat. Chem.* **2023**, *15* (4), 550−559.
(55) Garry, O. L.; Heilmann, M.; Chen, J.; Liang, Y.; Zhang, X.; Ma, X.; Yeung, C. S.; Bennett, D. J.; MacMillan, D. W. Rapid access to 2-substituted bicyclo [1.1. 1] pentanes. *J. Am. Chem. Soc.* **2023**, *145* (5), 3092−3100.
(56) Yang, Y.; Tsien, J.; Dykstra, R.; Chen, S.-J.; Wang, J. B.; Merchant, R. R.; Hughes, J. M. E.; Peters, B. K.; Gutierrez, O.; Qin, T. Programmable late-stage functionalization of bridge-substituted bicyclo[1.1.1]pentane bis-boronates. *Nat. Chem.* **2024**, *16* (2), 285−293.
(57) Hu, C.; Tsien, J.; Chen, S.-J.; Kong, M.; Merchant, R. R.; Kanda, Y.; Qin, T. A General Three-Component Alkyl Petasis Boron−Mannich Reaction. *J. Am. Chem. Soc.* **2024**, *146* (31), 21769−21777.
(58) Tsien, J.; Yang, Y. Y.; Valle, R. G. D.; Hughes, J. M. E.; Peters, B. K.; Merchant, R. R.; Qin, T. Intramolecular coupling for general synthesis of backbone substituted bicyclo[1.1.1]pentyl boronates. *Org. Synth.* **2024**, *101*, 181−206.
(59) Akinc, A.; Maier, M. A.; Manoharan, M.; Fitzgerald, K.; Jayaraman, M.; Barros, S.; Ansell, S.; Du, X.; Hope, M. J.; Madden, T. D.; Mui, B. L.; Semple, S. C.; Tam, Y. K.; Ciufolini, M.; Witzigmann, D.; Kulkarni, J. A.; van der Meel, R.; Cullis, P. R. The Onpattro story and the clinical translation of nanomedicines containing nucleic acid-based drugs. *Nat. Nanotechnol.* **2019**, *14* (12), 1084−1087.
(60) Xu, Y.; Golubovic, A.; Xu, S.; Pan, A.; Li, B. Rational design and combinatorial chemistry of ionizable lipids for RNA delivery. *J. Mater. Chem. B* **2023**, *11* (28), 6527−6539.
(61) Zhi, D.; Bai, Y.; Yang, J.; Cui, S.; Zhao, Y.; Chen, H.; Zhang, S. A review on cationic lipids with different linkers for gene delivery. *Adv. Colloid Interface Sci.* **2018**, *253*, 117−140.
(62) Dong, Y.; Siegwart, D. J.; Anderson, D. G. Strategies, design, and chemistry in siRNA delivery systems. *Adv. Drug Delivery Rev.* **2019**, *144*, 133−147.
(63) Lee, S. M.; Cheng, Q.; Yu, X.; Liu, S.; Johnson, L. T.; Siegwart, D. J. A systematic study of unsaturation in lipid nanoparticles leads to improved mRNA transfection in vivo. *Angew. Chem., Int. Ed.* **2021**, *60* (11), 5848−5853.
(64) Wang, X.; Liu, S.; Sun, Y.; Yu, X.; Lee, S. M.; Cheng, Q.; Wei, T.; Gong, J.; Robinson, J.; Zhang, D.; Lian, X.; Basak, P.; Siegwart, D. J. Preparation of selective organ targeting (SORT) lipid nanoparticles (LNPs) using multiple technical methods for tissue-specific mRNA delivery. *Nat. Protoc.* **2023**, *18* (1), 265−291.
(65) Wei, T.; Cheng, Q.; Min, Y.-L.; Olson, E. N.; Siegwart, D. J. Systemic nanoparticle delivery of CRISPR-Cas9 ribonucleoproteins for effective tissue specific genome editing. *Nat. Commun.* **2020**, *11* (1), 3232.
(66) Dilliard, S. A.; Cheng, Q.; Siegwart, D. J. On the mechanism of tissue-specific mRNA delivery by selective organ targeting nanoparticles. *Proc. Natl. Acad. Sci. U. S. A.* **2021**, *118* (52), No. e2109256118.
(67) Jayaraman, M.; Ansell, S. M.; Mui, B. L.; Tam, Y. K.; Chen, J. X.; Du, X. Y.; Butler, D.; Eltepu, L.; Matsuda, S.; Narayanannair, J. K.; Rajeev, K. G.; Hafez, I. M.; Akinc, A.; Maier, M. A.; Tracy, M. A.; Cullis, P. R.; Madden, T. D.; Manoharan, M.; Hope, M. J. Maximizing the potency of siRNA lipid nanoparticles for hepatic gene silencing in vivo. *Angew. Chem., Int. Ed.* **2012**, *51* (34), 8529−8533.
(68) Zheng, L.; Bandara, S. R.; Tan, Z.; Leal, C. Lipid nanoparticle topology regulates endosomal escape and delivery of RNA to the cytoplasm. *Proc. Natl. Acad. Sci. U. S. A.* **2023**, *120* (27), No. e2301067120.
(69) Preta, G. Development of new genome editing tools for the treatment of hyperlipidemia. *Cells* **2023**, *12* (20), 2466.
(70) Rothgangl, T.; Dennis, M. K.; Lin, P. J. C.; Oka, R.; Witzigmann, D.; Villiger, L.; Qi, W.; Hruzova, M.; Kissling, L.; Lenggenhager, D.; Borrelli, C.; Egli, S.; Frey, N.; Bakker, N.; Walker, J. A.; Kadina, A. P.; Victorov, D. V.; Pacesa, M.; Kreutzer, S.; Kontarakis, Z.; Moor, A.; Jinek, M.; Weissman, D.; Stoffel, M.; van Boxtel, R.; Holden, K.; Pardi, N.; Thöny, B.; Häberle, J.; Tam, Y. K.; Semple, S. C.; Schwank, G. In vivo adenine base editing of PCSK9 in macaques reduces LDL cholesterol levels. *Nat. Biotechnol.* **2021**, *39* (8), 949−957.

https://doi.org/10.1021/jacs.4c13154
J. Am. Chem. Soc. 2024, 146, 34733−34742